

PAPER • OPEN ACCESS

Seebeck effect in nanomagnets

To cite this article: Dmitry V Fedorov *et al* 2022 *J. Phys.: Condens. Matter* **34** 085801

View the [article online](#) for updates and enhancements.

You may also like

- [Probing topological quantum phase transitions via photonic spin Hall effects in spin-orbit coupled 2D quantum materials](#)
Muzamil Shah
- [Role of inelastic couplings in the \$^4\text{He} + ^{208}\text{Pb}\$ elastic scattering in a wide energy range](#)
Luiz Carlos Chamon, Leandro Romero Gasques and Juan Carlos Zamora Cardona
- [Active rheology in odd viscosity systems](#)
Cynthia J. Reichhardt and Charles Reichhardt



IOP | ebooks™

Bringing together innovative digital publishing with leading authors from the global scientific community.

Start exploring the collection—download the first chapter of every title for free.

Seebeck effect in nanomagnets

Dmitry V Fedorov^{1,2,3}, Martin Gradhand^{4,5,*} , Katarina Tauber²,
Gerrit E W Bauer^{6,7} and Ingrid Mertig^{2,3}

¹ Department of Physics and Materials Science, University of Luxembourg, L-1511 Luxembourg City, Luxembourg

² Institute of Physics, Martin Luther University Halle-Wittenberg, 06099 Halle, Germany

³ Max Planck Institute of Microstructure Physics, Weinberg 2, 06120 Halle, Germany

⁴ H H Wills Physics Laboratory, University of Bristol, Bristol BS8 1TL, United Kingdom

⁵ Institut für Physik, Johannes-Gutenberg-Universität Mainz, Staudingerweg 7, 55128 Mainz, Germany

⁶ WPI-AIMR and IMR and CSRN, Tohoku University, Sendai, Miyagi 980-8577, Japan

⁷ Zernike Institute for Advanced Materials, University of Groningen, Nijenborgh 4, 9747 AG Groningen, The Netherlands

E-mail: M.Gradhand@bristol.ac.uk

Received 16 September 2021, revised 5 November 2021

Accepted for publication 18 November 2021

Published 2 December 2021



CrossMark

Abstract

We present a theory of the Seebeck effect in nanomagnets with dimensions smaller than the spin diffusion length, showing that the spin accumulation generated by a temperature gradient strongly affects the thermopower. We also identify a correction arising from the transverse temperature gradient induced by the anomalous Ettingshausen effect and an induced spin-heat accumulation gradient. The relevance of these effects for nanoscale magnets is illustrated by *ab initio* calculations on dilute magnetic alloys.

Keywords: spin-dependent transport, transverse transport, spin-orbit coupling, Seebeck effect, DFT, Boltzmann equation, semiclassical transport

(Some figures may appear in colour only in the online journal)

1. Introduction

Spin caloritronics [1–3] addresses the coupling between the spin and heat transport in small structures and devices. The effects addressed so far can be categorized into several groups [2]. The first group covers phenomena whose origin is not connected to spin-orbit coupling (SOC). *Nonrelativistic* spin caloritronics in magnetic conductors addresses thermoelectric effects in which motion of electrons in a thermal gradient drives spin transport, such as the spin-dependent Seebeck [4] and the reciprocal Peltier [5, 6] effect. Another group of phenomena is caused by SOC and belongs to *relativistic* spin

caloritronics [2] including the anomalous [7] and spin [8–12] Nernst effects.

The Seebeck effect [13] or thermopower stands for the generation of an electromotive force or gradient of the electrochemical potential μ by temperature gradients ∇T . The Seebeck coefficient S parameterizes the proportionality when the charge current j vanishes:

$$(\nabla\mu/e)_{j=0} = S\nabla T. \quad (1)$$


In the two-current model for spin-polarized systems, the thermopower of a magnetic metal reads

$$S = \frac{\sigma^+ S^+ + \sigma^- S^-}{\sigma^+ + \sigma^-}, \quad (2)$$

where σ^\pm and S^\pm are the spin-resolved longitudinal conductivities and Seebeck coefficients, respectively.

Here, we study the Seebeck effect in nanoscale magnets on scales equal or less than their spin diffusion length [14]

* Author to whom any correspondence should be addressed.

 Original content from this work may be used under the terms of the [Creative Commons Attribution 4.0 licence](https://creativecommons.org/licenses/by/4.0/). Any further distribution of this work must maintain attribution to the author(s) and the title of the work, journal citation and DOI.

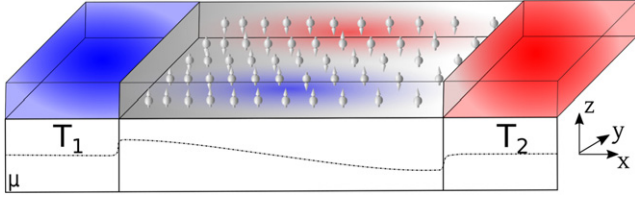


Figure 1. We consider a ferromagnetic metal slab smaller than the spin diffusion length in contact with two thermal baths hot (red) and cold (blue) that generate a temperature gradient in the x direction. The spheres with arrows represent the excited electrons with spin up and down parallel to the magnetization. The thermally induced electrons are represented by their density as well as a gradient in the grey scale of the background. The red and blue clouds indicate transverse heat accumulation (in the y direction). The dash-dotted line is the chemical potential μ for a high interface resistance to the contacts.

as in figure 1. Thermal baths on both sides of the sample drive a heat current in the x direction. Since no charge current flows, a thermovoltage builds up at the sample edges that can be observed non-invasively by tunnel junctions or scanning probes. Note that metallic contacts can detect the thermovoltage at zero-current bias conditions, but this requires additional modelling of the interfaces. We show in the following that in the presence of a thermally generated spin accumulation the thermopower differs from equation (2). We then focus on dilute ternary alloys of a Cu host with magnetic Mn and non-magnetic Ir impurities. By varying the alloy concentrations we may tune to the unpolarized case $S^+ = S^-$, as well as to spin-dependent S^+ and S^- parameters with equal or opposite signs. The single-electron thermoelectric effects considered here can be distinguished from collective magnon drag effects [15] by their temperature dependence.

2. Theory

In the two-current model of spin transport in a single-domain magnet [16–18], extended to include heat transport, the charge (\mathbf{j}) and heat (\mathbf{q}) current densities read

$$\mathbf{j}^\pm = \hat{\sigma}^\pm(\nabla\mu^\pm/e) - \hat{\sigma}^\pm\hat{S}^\pm\nabla T^\pm, \quad (3)$$

$$\mathbf{q}^\pm = \hat{\sigma}^\pm\hat{S}^\pm T(\nabla\mu^\pm/e) - \hat{\kappa}^\pm\nabla T^\pm, \quad (4)$$

where $\hat{\sigma}^\pm$, \hat{S}^\pm , and $\hat{\kappa}^\pm$ are the spin-resolved electric conductivity, Seebeck coefficient, and heat conductivity, respectively. All transport coefficients are tensors that reflect crystalline symmetry and SOC. The ‘four-current model’ equations (3) and (4) can be rewritten as

$$\begin{pmatrix} \mathbf{j} \\ \mathbf{j}^s \\ \mathbf{q} \\ \mathbf{q}^s \end{pmatrix} = \begin{pmatrix} \hat{\sigma} & \hat{\sigma}^s & \hat{\sigma}\hat{S}T & \hat{\sigma}\hat{S}^sT \\ \hat{\sigma}^s & \hat{\sigma} & \hat{\sigma}\hat{S}^sT & \hat{\sigma}\hat{S}T \\ \hat{\sigma}\hat{S}T & \hat{\sigma}\hat{S}^sT & \hat{\kappa}T & \hat{\kappa}^sT \\ \hat{\sigma}\hat{S}^sT & \hat{\sigma}\hat{S}T & \hat{\kappa}^sT & \hat{\kappa}T \end{pmatrix} \begin{pmatrix} \nabla\mu/e \\ \nabla\mu^s/2e \\ -\nabla T/T \\ -\nabla T^s/2T \end{pmatrix} \quad (5)$$

in terms of the charge $\mathbf{j} = \mathbf{j}^+ + \mathbf{j}^-$, spin $\mathbf{j}^s = \mathbf{j}^+ - \mathbf{j}^-$, heat $\mathbf{q} = \mathbf{q}^+ + \mathbf{q}^-$, and spin-heat $\mathbf{q}^s = \mathbf{q}^+ - \mathbf{q}^-$ current densities. Here, we introduced the conductivity tensors for charge

$\hat{\sigma} = \hat{\sigma}^+ + \hat{\sigma}^-$, spin $\hat{\sigma}^s = \hat{\sigma}^+ - \hat{\sigma}^-$, heat $\hat{\kappa} = \hat{\kappa}^+ + \hat{\kappa}^-$, and spin heat $\hat{\kappa}^s = \hat{\kappa}^+ - \hat{\kappa}^-$. The driving forces are

$$\nabla\mu = \frac{1}{2}(\nabla\mu^+ + \nabla\mu^-), \quad \nabla T = \frac{1}{2}(\nabla T^+ + \nabla T^-) \quad (6)$$

and the gradients of the spin $\mu^s = \mu^+ - \mu^-$ [18–21] and spin-heat $T^s = T^+ - T^-$ accumulations [2, 22–27]

$$\mu^s = \frac{1}{2}(\nabla\mu^+ - \nabla\mu^-), \quad \nabla T^s = \frac{1}{2}(\nabla T^+ - \nabla T^-). \quad (7)$$

Finally, the tensors

$$\hat{S} = \hat{\sigma}^{-1}(\hat{\sigma}^+\hat{S}^+ + \hat{\sigma}^-\hat{S}^-) \quad (8)$$

and

$$\hat{S}^s = \hat{\sigma}^{-1}(\hat{\sigma}^+\hat{S}^+ - \hat{\sigma}^-\hat{S}^-) \quad (9)$$

in equation (5) describe the charge and spin-dependent Seebeck coefficients, respectively. In cubic systems the diagonal component S_{ii} , where i is the Cartesian component of the applied temperature gradient, reduces to the scalar thermopower equation (2).

3. Results

In the following we apply equation (5) to the Seebeck effect in nanoscale magnets assuming their size to be smaller than the spin diffusion length. In this case the spin-flip scattering may be disregarded [28]. We focus first on longitudinal transport and disregard ∇T^s . However, we also discuss transverse (Hall) effects as well as the spin temperature gradient below. We adopt open-circuit conditions for charge and spin transport under a temperature gradient. Charge currents and, since we disregard spin-relaxation, spin currents vanish everywhere in the sample:

$$0 = \hat{\sigma}(\nabla\mu/e) + \hat{\sigma}^s(\nabla\mu^s/2e) - \hat{\sigma}\hat{S}\nabla T, \quad (10)$$

$$0 = \hat{\sigma}^s(\nabla\mu/e) + \hat{\sigma}(\nabla\mu^s/2e) - \hat{\sigma}\hat{S}^s\nabla T, \quad (11)$$

$$\mathbf{q} = T\hat{\sigma}[\hat{S}(\nabla\mu/e) + \hat{S}^s(\nabla\mu^s/2e)] - \hat{\kappa}\nabla T. \quad (12)$$

The thermopower now differs from the conventional expression given by equation (2). Let us introduce the tensor $\hat{\Sigma}$ as

$$\left. \frac{\nabla\mu}{e} \right|_{j=0} = \hat{\Sigma}\nabla T. \quad (13)$$

From equations (10) and (11), we find

$$\hat{\Sigma} = (\hat{\sigma} - \hat{\sigma}^s\hat{\sigma}^{-1}\hat{\sigma}^s)^{-1}(\hat{\sigma}\hat{S} - \hat{\sigma}^s\hat{S}^s). \quad (14)$$

When the spin accumulation in equation (10) vanishes we recover $\hat{\Sigma} \rightarrow \hat{S}$. Equation (14) involves only directly measurable material parameters [29], but the physics is clearer in the compact expression

$$\hat{\Sigma} = (\hat{S}^+ + \hat{S}^-)/2. \quad (15)$$

The spin polarization of the Seebeck coefficient

$$\left. \frac{\nabla \mu^s}{2e} \right|_{j=0} = \hat{\Sigma}^s \nabla T, \quad (16)$$

reads

$$\hat{\Sigma}^s = (\hat{\sigma} - \hat{\sigma}^s \hat{\sigma}^{-1} \hat{\sigma}^s)^{-1} (\hat{\sigma} \hat{S}^s - \hat{\sigma}^s \hat{S}), \quad (17)$$

or

$$\hat{\Sigma}^s = (\hat{S}^+ - \hat{S}^-)/2. \quad (18)$$

The diagonal elements of $\hat{\Sigma}$ govern the thermovoltage in the direction of the temperature gradient. The off-diagonal elements of $\hat{\Sigma}$ represent transverse thermoelectric phenomena such as the anomalous [7] and planar [30] Nernst effects. The diagonal and off-diagonal elements of $\hat{\Sigma}^s$ describe the spin-dependent Seebeck effect [2, 4], as well as (also in non-magnetic systems) the spin and planar-spin Nernst effects [8–12], respectively. We do not address here anomalous and Hall transport in the purely charge and heat sectors of equation (5).

3.1. Longitudinal spin accumulation

A temperature gradient in x direction $\nabla T \parallel \mathbf{e}_x$ induces the voltage in the same direction:

$$(\nabla_x \mu/e)_{j=0} = \Sigma_{xx} \nabla_x T. \quad (19)$$

In order to assess the importance of the difference between equations (14) and (15) and the conventional thermopower equation (2) we carried out first-principles transport calculations for the ternary alloys $\text{Cu}_{1-w}(\text{Mn}_{1-w}\text{Ir}_w)_v$, where $w \in [0, 1]$ and the total impurity concentration is fixed to $v = 1$ at.% [31]. We have chosen this system as a generic example where the Cu host ensures a reasonably large spin diffusion length and the two impurities allow us to scale easily between the different limits of strong spin-dependent scattering induced by magnetism for Cu(Mn) and SOC for Cu(Ir). The derived expressions equally apply to more conventional ferromagnets as long the dimensions of the sample is comparable or smaller than the spin diffusion length. We calculate the transport properties from the solutions of the linearized Boltzmann equation with collision terms calculated for isolated impurities [32, 33]. We disregard spin-flip scattering [33], which limits the size of the systems for which our results hold (see below). We calculate the electronic structure of the Cu host by the relativistic Korringa–Kohn–Rostoker method [34]. Figure 2 summarizes the calculated room-temperature (charge) thermopower equation (8) or (14) and (15) and their spin-resolved counterparts, equations (17) and (18). Table 1 contains additional information for the binary alloys Cu(Mn) and Cu(Ir) with $w = 0$ or $w = 1$ in figure 2, respectively. Here we implicitly assume an applied magnetic field that orders all localized moments.

We observe large differences (even sign changes) between S_{xx}^+ and S_{xx}^- that causes significant differences between $\Sigma_{xx} = (S_{xx}^+ + S_{xx}^-)/2$ and the macroscopic S_{xx} . The complicated behavior of the latter is caused by the weighting of

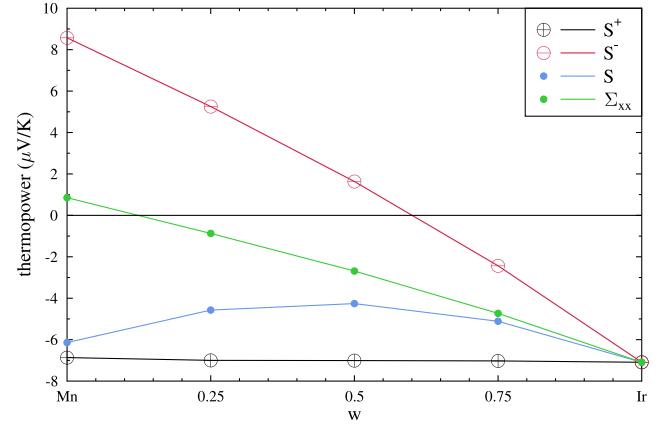


Figure 2. The diagonal thermopowers S and Σ , equations (8) and (14), respectively, as well as the spin-resolved thermopowers S^\pm as calculated for dilute $\text{Cu}(\text{Mn}_{1-w}\text{Ir}_w)$ alloys at 300 K with the total impurity concentration 1 at.%.

Table 1. Computed spin-resolved and charge thermopowers as defined in the text for magnetic $\text{Cu}_{0.99}\text{Mn}_{0.01}$ and $\text{Cu}_{0.99}(\text{Mn}_{0.5}\text{Ir}_{0.5})_{0.01}$ as well as non-magnetic $\text{Cu}_{0.99}\text{Ir}_{0.01}$ dilute alloys. The conventional spin Seebeck coefficient is shown for comparison. All quantities are calculated at 300 K in units of $\mu\text{V K}^{-1}$.

System	$\text{Cu}_{0.99}\text{Mn}_{0.01}$	$\text{Cu}_{0.99}(\text{Mn}_{0.5}\text{Ir}_{0.5})_{0.01}$	$\text{Cu}_{0.99}\text{Ir}_{0.01}$
S_{xx}^+	-6.87	-7.01	-7.09
S_{xx}^-	8.57	1.64	-7.09
S_{xx}	-6.14	-4.26	-7.09
Σ_{xx}	0.85	-2.69	-7.09
Σ_{xx}^s	-7.72	-4.33	0.00

S^+ and S^- by the corresponding conductivities, see equation (8). Even though a spin-accumulation gradient suppresses the Seebeck effect, an opposite sign of S_{xx}^+ and S_{xx}^- can enhance Σ_{xx}^s beyond the microscopic as well as macroscopic thermopower. Indeed, Hu *et al* [35] observed a spin-dependent Seebeck effect that is larger than the charge Seebeck effect in CoFeAl. Our calculations illustrate that the spin-dependent Seebeck effect can be engineered and maximized by doping a host material with impurities.

3.2. Hall transport

In the presence of spin-orbit interactions the applied temperature gradient ∇T_{ext} induces anomalous Hall currents. When the electron-phonon coupling is weak, the spin-orbit interaction can, for example, induce transverse temperature gradients. In a cubic magnet the charge and spin conductivity tensors are antisymmetric. With magnetization and spin quantization axis along z :

$$\hat{\sigma}^{(s)} = \begin{pmatrix} \sigma_{xx}^{(s)} & -\sigma_{yx}^{(s)} & 0 \\ \sigma_{yx}^{(s)} & \sigma_{xx}^{(s)} & 0 \\ 0 & 0 & \sigma_{zz}^{(s)} \end{pmatrix}, \quad (20)$$

and analogous expressions hold for \hat{S} and \hat{S}^s . A charge current in the x direction generates a transverse heat current that heats and cools opposite edges, respectively. A transverse temperature gradient $\nabla T_{\text{ind}} \parallel \mathbf{e}_y$ is signature of this anomalous Ettingshausen effect [36] gradient. From equations (12), (13), and (16)

$$\mathbf{q} = \left[T\hat{\sigma}(\hat{S}\hat{\Sigma} + \hat{S}^s\hat{\Sigma}^s) - \hat{\kappa} \right] \nabla T, \quad (21)$$

where $\nabla T = \mathbf{e}_x \nabla_x T_{\text{ext}} + \mathbf{e}_y \nabla_y T_{\text{ind}}$. Assuming weak electron-phonon scattering, the heat cannot escape the electron systems and $q_y = 0$. equation (21) then leads to

$$\nabla_y T_{\text{ind}} = -\frac{A_{yx}}{A_{yy}} \nabla_x T_{\text{ext}}, \quad (22)$$

where A_{yx} and A_{yy} are components of the tensor

$$\hat{A} = T\hat{\sigma}(\hat{S}\hat{\Sigma} + \hat{S}^s\hat{\Sigma}^s) - \hat{\kappa}. \quad (23)$$

Consequently, equation (13) leads to a correction to the thermopower

$$(\nabla_x \mu/e)_{j=0} = \left[\Sigma_{xx} - \Sigma_{xy} \frac{A_{yx}}{A_{yy}} \right] \nabla_x T_{\text{ext}}. \quad (24)$$

However, this effect should be small [37–40] for all but the heaviest elements but may become observable when Σ_{xx} vanishes, which according to figure 2 should occur at around $w = 0.125$.

3.3. Spin temperature gradient

At low temperatures, the spin temperature gradient ∇T^s may persist over length scales smaller but of the same order as the spin accumulation [25]. From equations (3), (15), and (18) it follows

$$(\nabla \mu/e)_{j=0} = \hat{\Sigma} \nabla T + \hat{\Sigma}^s \nabla T^s / 2, \quad (25)$$

$$(\nabla \mu^s / 2e)_{j=0} = \hat{\Sigma}^s \nabla T + \hat{\Sigma} \nabla T^s / 2. \quad (26)$$

Starting with equation (5) and employing equations (25) and (26) for the heat and spin-heat current densities we obtain

$$\mathbf{q} = \hat{A} \nabla T + \hat{B} \nabla T^s / 2 \quad \text{and} \quad \mathbf{q}^s = \hat{B} \nabla T + \hat{A} \nabla T^s / 2, \quad (27)$$

where

$$\hat{B} = T\hat{\sigma}(\hat{S}\hat{\Sigma}^s + \hat{S}^s\hat{\Sigma}) - \hat{\kappa}^s, \quad (28)$$

and \hat{A} is defined by equation (23). With $\nabla T^s = \mathbf{e}_y \nabla_y T_{\text{in}}^s$ and $\nabla T = \mathbf{e}_x \nabla_x T_{\text{ex}} + \mathbf{e}_y \nabla_y T_{\text{in}}$ we find

$$\begin{aligned} (\nabla_x \mu/e)_{j=0} &= \Sigma_{xx} \nabla_x T_{\text{ex}} + \Sigma_{xy} \nabla_y T_{\text{in}} + \Sigma_{xy}^s \nabla_y T_{\text{in}}^s / 2 \\ &= \left[\Sigma_{xx} - \Sigma_{xy} \frac{A_{yy} A_{yx} - B_{yy} B_{yx}}{A_{yy} A_{yy} - B_{yy} B_{yy}} \right. \\ &\quad \left. - \Sigma_{xy}^s \frac{A_{yy} B_{yx} - B_{yy} A_{yx}}{A_{yy} A_{yy} - B_{yy} B_{yy}} \right] \nabla_x T_{\text{ex}} \end{aligned} \quad (29)$$

assuming again $q_y = 0$ and $q_y^s = 0$. Similar to equation (24), the Hall corrections in equation (29) should be significant only when Σ_{xx} vanishes for $w = 0.125$. However, experimentally it might be difficult to separate the thermopowers equations (29) and (24).

3.4. Spin diffusion length and mean free path

Our first-principles calculation are carried out for bulk dilute alloys based on Cu and in the single site approximation of spin-conserving impurity scattering. The Hall effects are therefore purely extrinsic. This is an approximation that holds on length scales smaller than various spin diffusion lengths l_{sf} . On the other hand, the Boltzmann equation approach is valid when the sample is larger than the elastic scattering mean free path l , so our results should be directly applicable for sample lengths L that fulfill $l < L \leq l_{\text{sf}}$. According to references [37, 40], for the ternary alloy Cu(Mn_{0.5}Ir_{0.5}) with impurity concentration of 1 at.% the present results hold on length scales 26 nm $< L \leq 60$ nm and 100 nm $< L \leq 400$ nm for Cu(Mn). On the other hand, for nonmagnetic Cu(Ir) the applicability is limited to a smaller interval 10 nm $< L \leq 16$ nm. We believe that while the results outside these strict limits may not be quantitatively reliable, they still give useful insights into trends.

4. Summary and outlook

In summary, we derived expressions for the thermopower valid for ordered magnetic alloys for sample sizes that do not exceed the spin diffusion lengths (that have to be calculated separately). We focus on dilute alloys of Cu with Mn and Ir impurities. For 1% ternary alloys Cu(Mn_{1-w}Ir_w) with $w < 0.5$ the spin diffusion length is $l_{\text{sf}} > 60$ nm. In this regime the spin and charge accumulations induced by an applied temperature gradient strongly affect each other. By *ab initio* calculations of the transport properties of Cu(Mn_{1-w}Ir_w) alloys, we predict thermopowers that drastically differ from the bulk value even changing sign. Relativistic Hall effects generate spin accumulations normal to the applied temperature gradient that become significant when the longitudinal thermopower Σ_{xx} vanishes, for example for Cu(Mn_{1-w}Ir_w) alloys at $w \approx 0.125$.

After having established the principle existence of the various corrections to the conventional transport description it would be natural to move forward to describe extended thin films. A first-principles version of the Boltzmann equation including all electronic spin non-conserving scatterings in extended films is possible, but very expensive for large l_{sf} . It would still be incomplete, since the relaxation of heat to the lattice by electron-phonon interactions and spin-heat by electron–electron scattering [23, 24] are not included. We therefore propose to proceed pragmatically: The regime $l < l_{\text{sf}} < L$ is accessible to spin-heat diffusion equations that can be parameterized by first-principles material-dependent parameters as presented here and relaxation lengths that may be determined otherwise, such as by fitting to experimental results.

Acknowledgments

This work was partially supported by the Deutsche Forschungsgemeinschaft via SFB 762 and the priority program SPP 1538 as well as JSPS Grants-in-Aid for Scientific Research (KAKENHI Grant No. 19H00645). MG

acknowledges financial support from the Leverhulme Trust via an Early Career Research Fellowship (ECF-2013-538) and a visiting professorship at the Centre for Dynamics and Topology of the Johannes-Gutenberg-University Mainz.

Data availability statement

The data that support the findings of this study are available upon reasonable request from the authors.

ORCID iDs

Martin Gradhand  <https://orcid.org/0000-0003-3780-4646>

References

- [1] Bauer G E W, MacDonald A H and Maekawa S 2010 ‘Spin caloritronics’ *Solid State Commun.* **150** 459
- [2] Bauer G E W, Saitoh E and van Wees B J 2012 Spin caloritronics *Nat. Mater.* **11** 391
- [3] Boona S R, Myers R C and Heremans J P 2014 Spin caloritronics *Energy Environ. Sci.* **7** 885
- [4] Slachter A, Bakker F L, Adam J-P and van Wees B J 2010 Thermally driven spin injection from a ferromagnet into a non-magnetic metal *Nat. Phys.* **6** 879
- [5] Flipse J, Bakker F L, Slachter A, Dejene F K and van Wees B J 2012 Direct observation of the spin-dependent Peltier effect *Nat. Nanotechnol.* **7** 166
- [6] Gönnerwein S and Bauer G E W 2012 Electron spins blow hot and cold *Nat. Nanotechnol.* **7** 145
- [7] Miyasato T, Abe N, Fujii T, Asamitsu A, Onoda S, Onose Y, Nagaosa N and Tokura Y 2007 Crossover behavior of the anomalous Hall effect and anomalous Nernst effect in itinerant ferromagnets *Phys. Rev. Lett.* **99** 086602
- [8] Cheng S-G, Xing Y, Sun Q-F and Xie X C 2008 Spin Nernst effect and Nernst effect in two-dimensional electron systems *Phys. Rev. B* **78** 045302
- [9] Liu X and Xie X C 2010 Spin Nernst effect in the absence of a magnetic field *Solid State Commun.* **150** 471
- [10] Ma Z 2010 Spin Hall effect generated by a temperature gradient and heat current in a two-dimensional electron gas *Solid State Commun.* **150** 510
- [11] Tauber K, Gradhand M, Fedorov D V and Mertig I 2012 Extrinsic spin Nernst effect from first principles *Phys. Rev. Lett.* **109** 026601
- [12] Bose A and Tulapurkar A A 2019 Recent advances in the spin Nernst effect *J. Magn. Magn. Mater.* **491** 165526 and references therein
- [13] Seebeck T J 1822 *Magnetische Polarisation der Metalle und Erze durch Temperatur-Differenz* (Berlin: Abhandlungen der Königlichen Akademie der Wissenschaften) pp 265–373
- [14] Systems with dimensions larger than the spin-flip length require the solution of a spin-heat diffusion problem [28].
- [15] Watzman S J, Duine R A, Tserkovnyak Y, Boona S R, Jin H, Prakash A, Zheng Y and Heremans J P 2016 Magnon-drag thermopower and Nernst coefficient in Fe, Co, and Ni *Phys. Rev. B* **94** 144407
- [16] Mott N F 1936 The electrical conductivity of transition metals *Proc. R. Soc. A* **153** 699
- [17] Fert A and Campbell I A 1968 Two-current conduction in nickel *Phys. Rev. Lett.* **21** 1190
- [18] van Son P C, van Kempen H and Wyder P 1987 Boundary resistance of the ferromagnetic–nonferromagnetic metal interface *Phys. Rev. Lett.* **58** 2271
- [19] Johnson M and Silsbee R H 1987 Thermodynamic analysis of interfacial transport and of the thermomagnetolectric system *Phys. Rev. B* **35** 4959
- [20] Johnson M and Silsbee R H 1988 Ferromagnet–nonferromagnet interface resistance *Phys. Rev. Lett.* **60** 377
- [21] Valet T and Fert A 1993 Theory of the perpendicular magnetoresistance in magnetic multilayers *Phys. Rev. B* **48** 7099
- [22] Hatami M, Bauer G E W, Zhang Q and Kelly P J 2007 Thermal spin-transfer torque in magnetoelectronic devices *Phys. Rev. Lett.* **99** 066603
- [23] Heikkilä T T, Hatami M and Bauer G E W 2010 Spin heat accumulation and its relaxation in spin valves *Phys. Rev. B* **81** 100408
- [24] Heikkilä T T, Hatami M and Bauer G E W 2010 Electron–electron interaction induced spin thermalization in quasi-low-dimensional spin valves *Solid State Commun.* **150** 475
- [25] Dejene F K, Flipse J, Bauer G E W and van Wees B J 2013 Spin heat accumulation and spin-dependent temperatures in nanopillar spin valves *Nat. Phys.* **9** 636
- [26] Vera-Marun I J, van Wees B J and Jansen R 2014 Spin heat accumulation induced by tunneling from a ferromagnet *Phys. Rev. Lett.* **112** 056602
- [27] Wong C H, Stooft H T C and Duine R A 2015 Spin-heat relaxation and thermospin diffusion in atomic Bose and Fermi gases *Phys. Rev. A* **91** 043602
- [28] Hatami M, Bauer G E W, Takahashi S and Maekawa S 2010 Thermoelectric spin diffusion in a ferromagnetic metal *Solid State Commun.* **150** 480
- [29] \hat{S} and \hat{S}^s defined by equations (8) and (9) can be measured in samples much larger than the spin diffusion length.
- [30] Pu Y, Johnston-Halperin E, Awschalom D D and Shi J 2006 Anisotropic thermopower and planar Nernst effect in $\text{Ga}_{1-x}\text{Mn}_x\text{As}$ ferromagnetic semiconductors *Phys. Rev. Lett.* **97** 036601
- [31] Tauber K, Fedorov D V, Gradhand M and Mertig I 2013 Spin Hall and spin Nernst effect in dilute ternary alloys *Phys. Rev. B* **87** 161114(R)
- [32] Mertig I 1999 Transport properties of dilute alloys *Rep. Prog. Phys.* **62** 237
- [33] Gradhand M, Fedorov D V, Zahn P and Mertig I 2010 Extrinsic spin Hall effect from first principles *Phys. Rev. Lett.* **104** 186403
- [34] Gradhand M, Czerner M, Fedorov D V, Zahn P, Yavorsky B Y, Szunyogh L and Mertig I 2009 Spin polarization on Fermi surfaces of metals by the KKR method *Phys. Rev. B* **80** 224413
- [35] Hu S, Itoh H and Kimura T 2014 Efficient thermal spin injection using CoFeAl nanowire *NPG Asia Mater.* **6** e127
- [36] Hu S and Kimura T 2013 Anomalous Nernst–Ettingshausen effect in nonlocal spin valve measurement under high-bias current injection *Phys. Rev. B* **87** 014424
- [37] Gradhand M, Fedorov D V, Zahn P and Mertig I 2010 Spin Hall angle versus spin diffusion length: tailored by impurities *Phys. Rev. B* **81** 245109
- [38] Lowitzer S, Gradhand M, Ködderitzsch D, Fedorov D V, Mertig I and Ebert H 2011 Extrinsic and intrinsic contributions to the spin Hall effect of alloys *Phys. Rev. Lett.* **106** 056601
- [39] Gradhand M, Fedorov D V, Zahn P and Mertig I 2011 Skew scattering mechanism by an *ab initio* approach: extrinsic spin Hall effect in noble metals *Solid State Phenom.* **168–169** 27
- [40] Gradhand M, Fedorov D V, Zahn P, Mertig I, Otani Y, Niimi Y, Vila L and Fert A 2012 Perfect alloys for spin Hall current-induced magnetization switching *SPIN* **02** 1250010